HiSST: International Conference on
High-Speed Vehicle Science Technology
26–29 November 2018, Moscow, Russia

Optimum Trim of an Experimental Hypersonic Glider

Victor F. Villace[1], Sergey A. Takovitskii[2]

Abstract

Single point trimming of the hypersonic glider is not sufficient to accomplish the mission requirements and attain maximum performance. Applied to a hypersonic flight experiment, the present research shows that drifts of +/-4% around the centre of gravity imply large penalties on the aerodynamic efficiency along the intended glider trajectory, unless that the vehicle control is optimised for each particular case. The analysis is based on three degrees of freedom trajectory analysis and optimization.

Keywords: *trajectory, trim, optimization*

1. Introduction

A flight test vehicle is under design to demonstrate several of the critical technologies needed for sustained hypersonic flight [1]. The vehicle targets an autonomous guidance and control to demonstrate to an aerodynamic efficiency in excess of 4 and a supersonic glide down to Mach 2. The vehicle will be rocket launched to suborbital speed and, once stabilized by the cold gas system, will detach from the service nodule. The vehicle will then be free flying and will initiate a pull up manoeuvre. During this phase, the trimming of the aircraft is competing between the manoeuvrability required to carry on the pull up and stability, while at the same time the flight experiment should demonstrate a high aerodynamic performance during the gliding phase.

The focus of the current study is on determining the sensitivity of the trajectory to the location of the aircraft centre of gravity (CoG). Whereas the CoG position is established by design, the realization of the vehicle will carry on drifts of the CoG that will be measured and corrected with a ballast mass. Motivated by the encouraging reduction of trim drag by the use of ballast mass reported in [2], the current work evaluates the sensitivity of the trajectory performance to the CoG position and draws the optimal trajectories for each CoG drift.

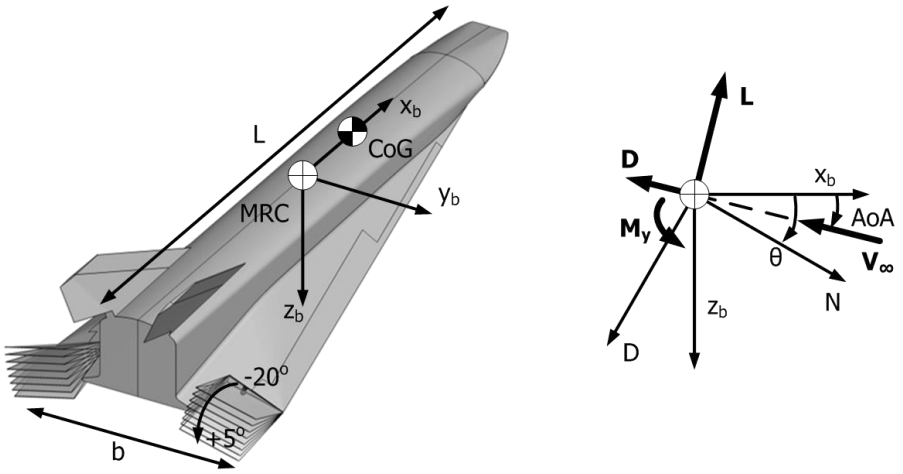

Fig 1. Overview of the EFTV body axes and aerodynamic forces

[1] *European Space Agency, the Netherlands, victor.villace@esa.int*
[2] *Central Aerohydrodynamic Institute (TsAGI), Russian Federation, c.a.t@tsagi.ru*

2. Methodology

The inviscid aerodynamic database of the experimental vehicle comprises the longitudinal and lateral-directional characteristics of the vehicle [3]. For the current purpose, solely the longitudinal coefficients of lift, drag and pitching moment are required. These are considered in the form of three-dimensional tables which are function of Mach number (Ma), angle-of-attack (AoA) and elevator deflection. For simplicity, the table granularity was reduced to Ma 2, 5, 7 and 9; AoA -6, 0, 6 and 16 degrees and elevator deflections of -20, -15, -10, -5, 0 and 6 degrees. The charts in Fig 2 show the longitudinal coefficients. The vehicle has a reference length (L) of 3.29 m, a span (b) of 1.24 m and a reference planform area of 2.52 m2. The moment reference centre (MRC) is located at a distance of 57% of the reference length from the nose tip.

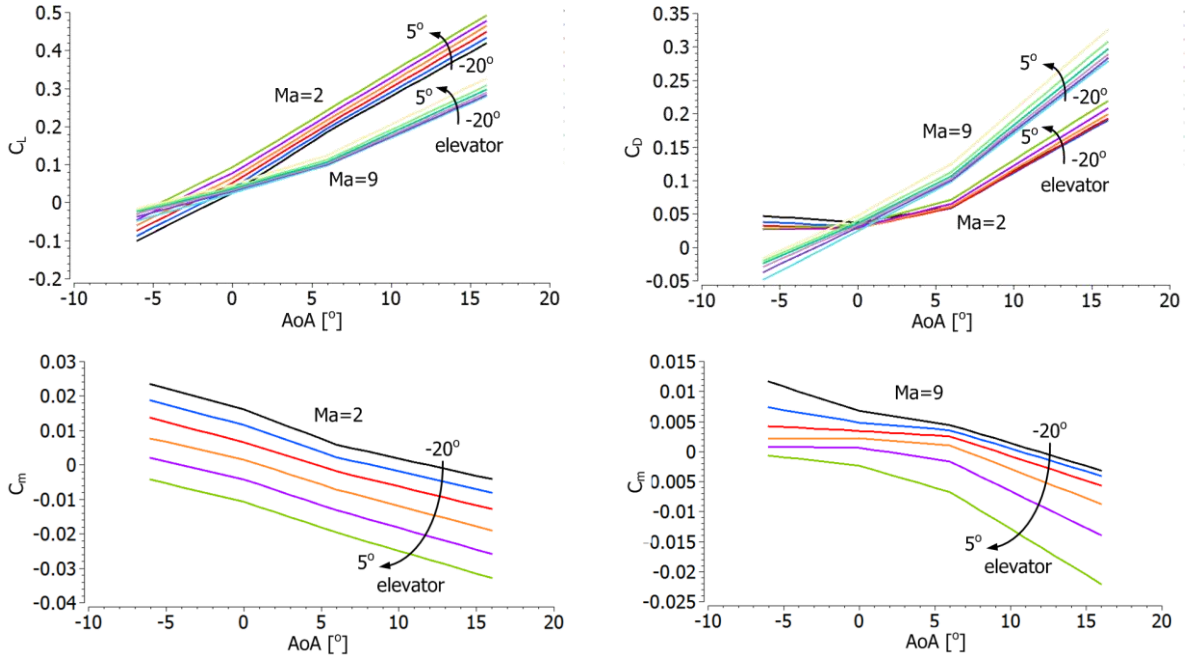

Fig 2. Longitudinal aerodynamic coefficients

The three degrees of freedom model of the aircraft was developed in EcosimPro by means of the flight simulation library [4]. The pitch rate is commanded to the autopilot in open loop, as a function of time. Default dynamics are considered for the actuation lane as well as for the dynamic derivatives pertaining to the vehicle aerodynamics. The trajectories were optimised by means of the population based stochastic algorithm solver, part of the optimization library of EcosimPro.

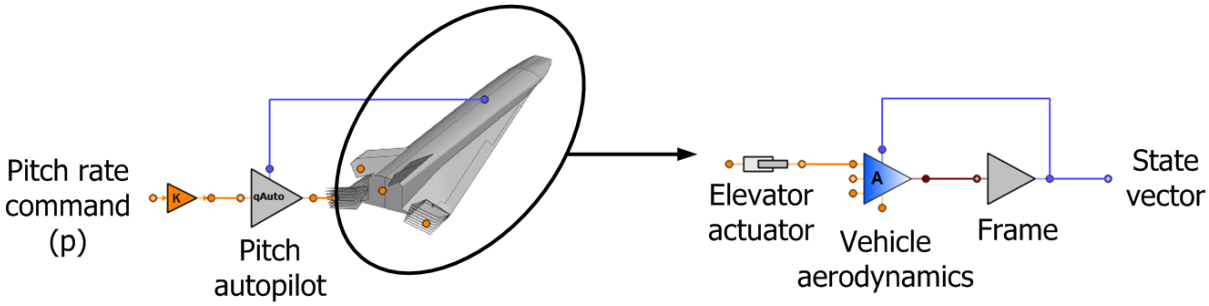

Fig 3. Schematic representation of the aircraft model

3. Results

3.1. Constant pitch rate

A null pitch rate is commanded to the autopilot throughout the descent flight. The CoG is at 58% from the nose tip. The vehicle mass is 464 kg and the moment of inertia along the Oy_b axis is 1402

kg m^2. The vehicle flies at Ma 6.1 and 50 km of altitude with null angle of attack and inclination (θ=0) when the simulation is started. Since levelled flight is not possible with this attitude and flight regime, the vehicle inclination oscillates initially while it evolves towards a steady condition. This is appreciated on the evolution of the aerodynamic efficiency and elevator deflection during the first seconds of flight, in Fig 4 and Fig 5.

Four simulations were performed to characterise the trajectory sensitivity to the ballast mass, in Table 1. The CoG shift refers to the position of the CoG with respect to the MRC. The nominal CoG corresponds to the current design target. Both backward and forward deviation of 4% where considered to quantify the sensitivity of the trajectory to the realised CoG positions. Finally, a ballast mass was used to relocate the CoG to the nominal position. In the worst case of a 4% forward drift, the ballast mass amounts to 11% of the vehicle mass. The ballast is located either 5% from the nose tip or 5% from the vehicle base, depending on the sense backward/forward of the CoG drift.

Table 1. Trajectory cases

Case	Vehicle mass [kg]	Mass increment [%]	CoG drift [%]
Nominal CoG	464	-	-0.9
Ballast	514	11	-0.9
Backward deviation	464	0	-4.9
Forward deviation	464	0	3.1

The results of Fig 4 show a clear decrease of the aerodynamic efficiency when the CoG drifts forward. The sudden drop takes place just as the vehicle comes out of the pull up manoeuvre, at around 100s into the flight. The reason for this is the increased elevator deflection angle needed to trim the vehicle. The backwards drift reduces the lift-to-drag ratio, nonetheless the trend is not as dramatic as for the forward drift. In fact, such trimming is beneficial towards the end of the mission with respect to the nominal case. The backwards drift requires an overall positive elevator deflection after the pull up, in Fig 5, which enables a larger aerodynamic efficiency than in the forward drift. The ballast trimmed vehicle exhibit the same performances as the nominal CoG case.

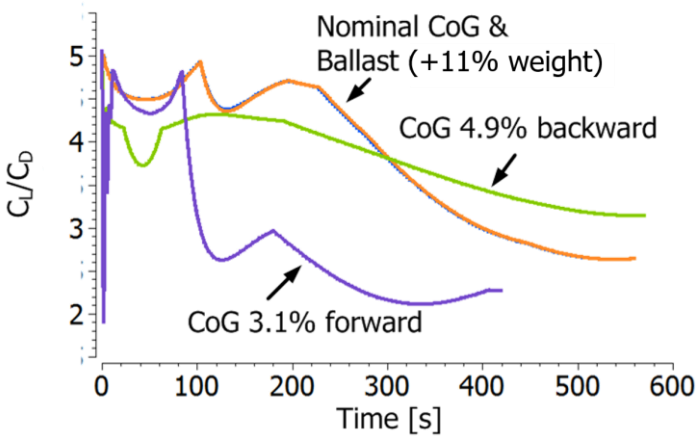

Fig 4. Aerodynamic efficiencies along the four trajectories

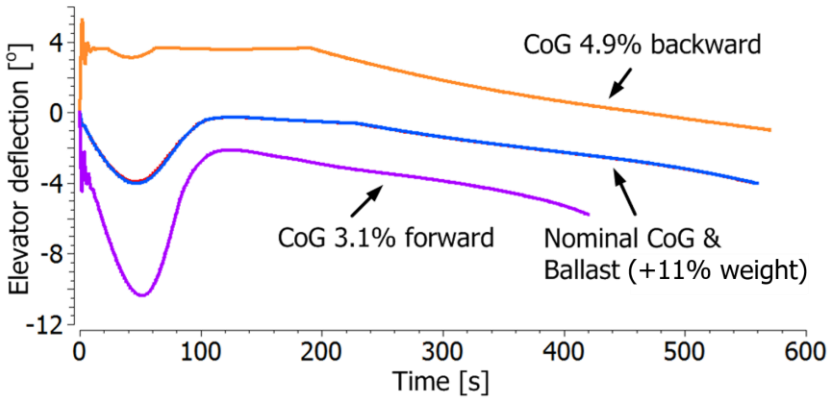

Fig 5. Elevator deflection angle along the four trajectories

Fig 6 and Fig 7 highlight a decrease of 30% and 25% in respectively flight time and downrange due to the CoG forward drift. On the other hand, the ballast-trimmed vehicle is able to perform as the nominal one, and the vehicle configuration is clearly more resilient to a backward than a forward CoG drift, performing almost as good as the nominally trimmed vehicle. The backward CoG position favours the pull up manoeuvre compared to the nominal and forward CoG positions. This is evident in Fig 5 by the lower elevator deflection required during the first 100s. Consequently, the backward CoG drift allows terminating the pull up earlier and at higher altitude than for the forward CoG drift.

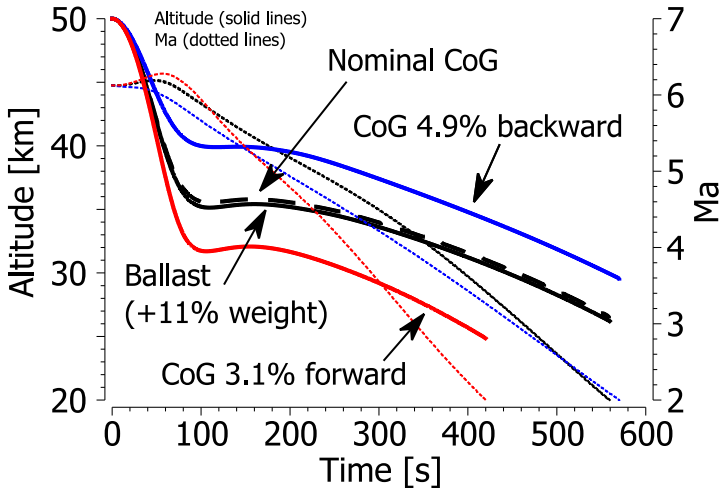

Fig 6. Altitude and Mach number along the four trajectories

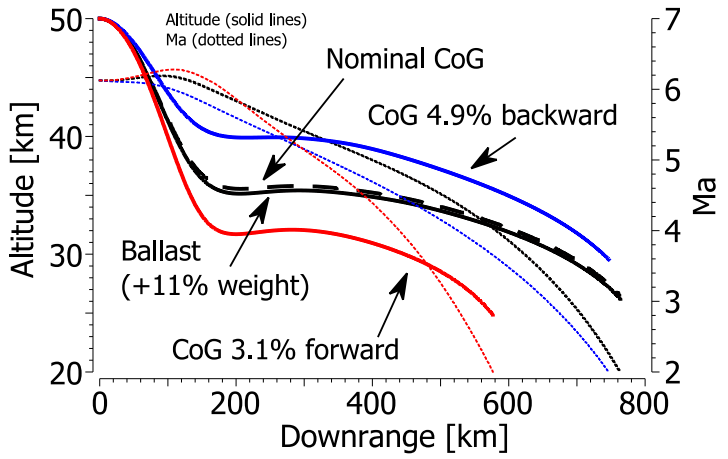

Fig 7. Altitude and Mach number vs. downrange along the four trajectories

3.2. Optimized pitch rate

The following vehicle mass, CoG and trajectory injection conditions are considered in the subsequent analyses:

- Vehicle mass: 400kg
- Nominal CoG: 59% from nose tip
- AoA: 3º
- Pitch angle (θ): -18.7º
- Altitude: 55km
- Flight path angle: -21.7º
- Flight path speed: 2334 m/s (V_{xb}=2331m/s, V_{zb}=122m/s)

As optimization variable, the pitch rate command is discretized into 11 control points: the first 7 points at 50 s intervals for a better capture of the pull up manoeuvre, the remaining 4 following 100 s time intervals. The optimization objective is to maximize the down range to Mach 2 and minimize the pitch angle. For the latter, the RMS of the pitch angle is used with the aim of eliminating the phugoid motion after the pull up. Since the method is single-objective, the cost function consist of a weighted sum of both penalties for the minimization problem. It was found that if a single penalty on pitch was used, then the optimizer strategy was to decrease the penalty by shortening the trajectories.

Four optimal trajectories are drawn corresponding to backward and forward CoG drifts ranging from -3% to 4% with regard to the nominal CoG. The vehicle becomes instable for a backward drift of -4%. Fig 8 shows that a null pitch angle of less than +/- 1º is achieved soon after the pull up manoeuvre.

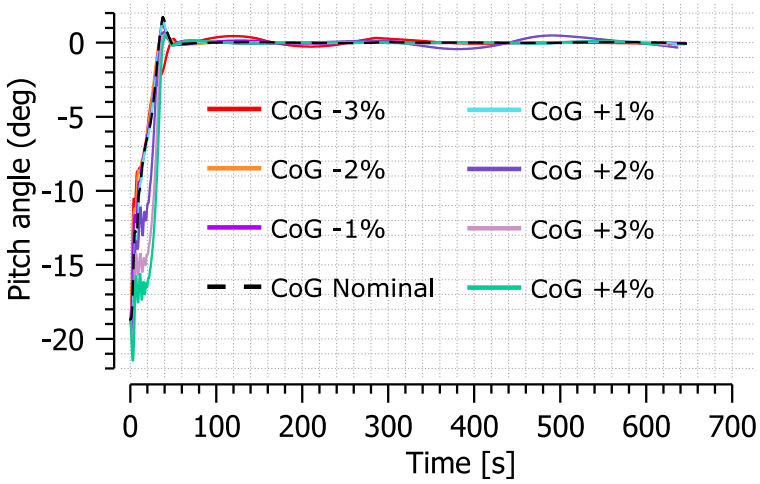

Fig 8. Pitch angle of optimised trajectories for various CoG positions.

The sensitivity analysis of §3.1 showed a 25% decrease of downrange when the CoG drifts 4% forwards. On the contrary, when the pitch command is optimized for each CoG position, a 4% drift of the CoG leads to less than 5% change of downrange. Moreover, Fig 9 shows that the trend is symmetrical: as the CoG drifts from the nominal position the downrange decreases. Nonetheless, the maximum speed prior pull up increases monotonically with forward drifts. The reason is that the vehicle starts losing pull up command at forward CoG drifts of 1%, as the aileron reaches the maximum negative deflection (Fig 10), with and unavoidably deeper plunge (Fig 11), increased velocity, dynamic pressure and aerodynamic hinge moment (Fig 12). The vehicle decelerates faster and hence cruises at a higher angle of attack and consequently lower aerodynamic efficiency, in Fig 13 and Fig 14. The latter reduces the downrange as compared to the backwards CoG positions.

On the contrary, for nominal and backwards CoG drifts, the vehicle gains authority to fly at higher angle of attack. The vehicle reaches soon the maximum angle of attack of 15º, and hence from this moment on, the dynamic pressure, aerodynamic efficiency and angle of attack do not vary considerably.

The importance of flying at nominal centre of gravity is justified by e.g. the necessity of maintaining a high aerodynamic efficiency or the survivability of the actuation lane to the elevator hinge moment. The need to weight-ballast the vehicle to correct the CoG drifts originating from manufacturing uncertainties is therefore obvious. A worst case of 2% forward CoG drift was considered, which results in a 6% weight increase to the additional ballast weight, in Table 2. The trajectory was optimized for the ballasted vehicle, subject to the same cost function as previously, and resulted in identical Mach number profiles and downrange for both the nominal and the ballasted vehicle, in Fig 15. The altitude profile was slightly lower for the ballasted vehicle since a deeper plunge was required. The deeper plunge is also noticed by the slight increase of peak dynamic pressure and elevator hinge moment, in Fig 16. The aerodynamic efficiency, angle of attack, elevator deflection and pitch angle are not shown, but resulted in identical profiles as those of the nominal vehicle.

Table 2. Ballast masses

CoG Drift	Ballast mass [kg]	Ballast to vehicle mass [%]
1% forward	11	3
2% forward	22	6
1% backward	7	2
2% backward	15	4

In line with the preliminary results in §3.1, the down range is little sensitive to the ballast mass. In fact a 6% increase in mass imply the same increase in insertion energy (kinetic and potential), since the initial altitude and speed are maintained constant in our analysis. Nonetheless, the increased drag progressively takes over the extra insertion energy. This is evident in the energy and irreversibility profiles, in Fig 17, where both nominal and ballast corrected trajectory finalise at nearly the same energy level. The irreversibility is the work of the drag force.

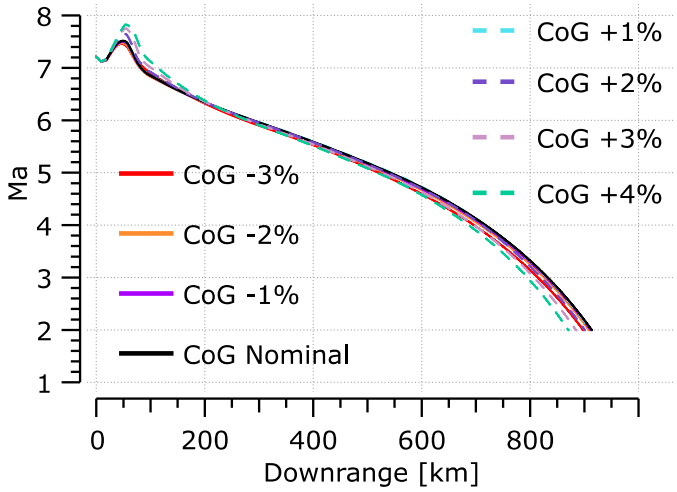

Fig 9. Mach of optimised trajectories for various CoG positions.

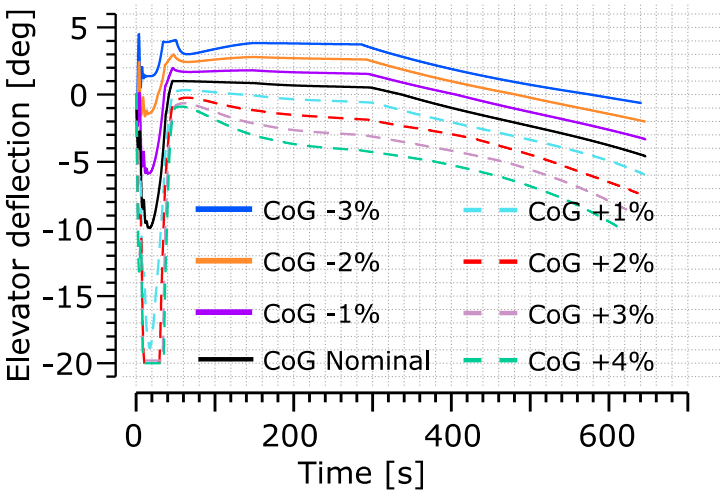

Fig 10. Elevator deflection of optimised trajectories for various CoG positions.

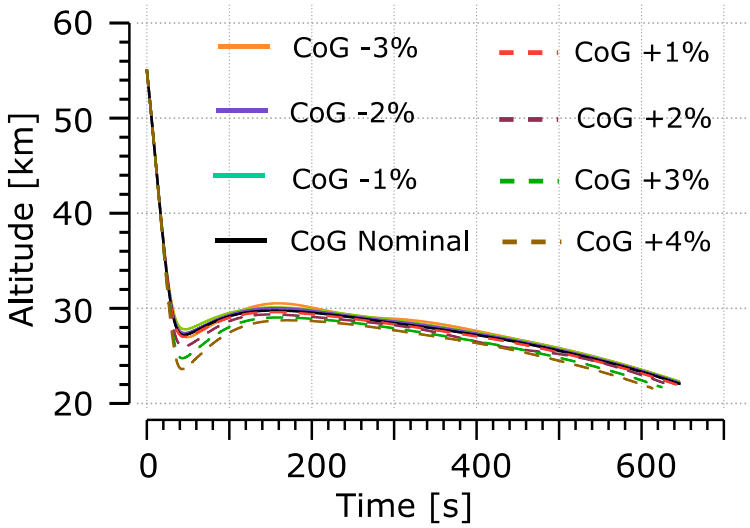

Fig 11. Altitude profile of optimised trajectories for various CoG positions.

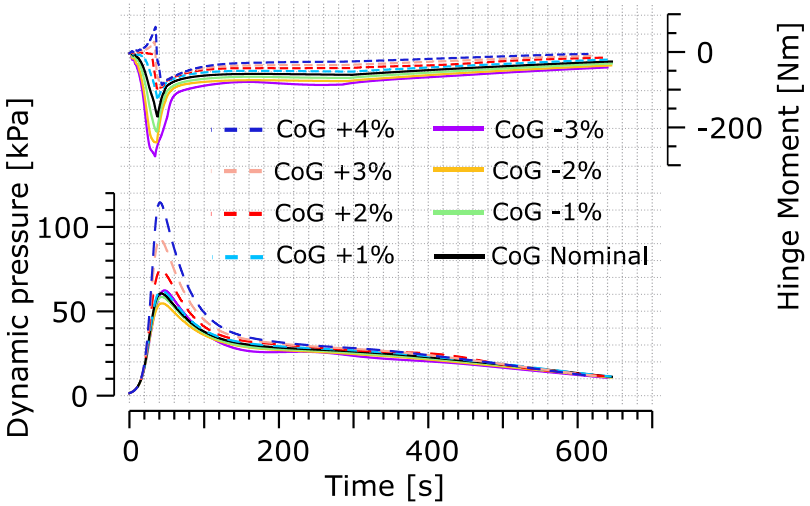

Fig 12. Dynamic pressure and elevator hinge moment of optimised trajectories for various CoG positions.

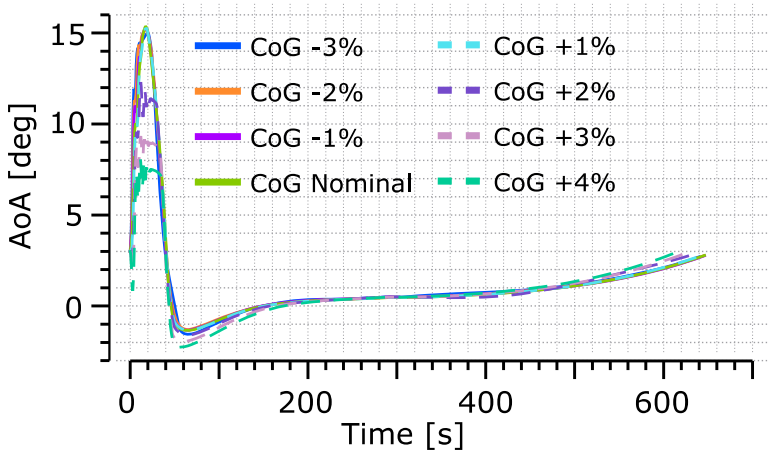

Fig 13. Angle of attack of optimised trajectories for various CoG positions.

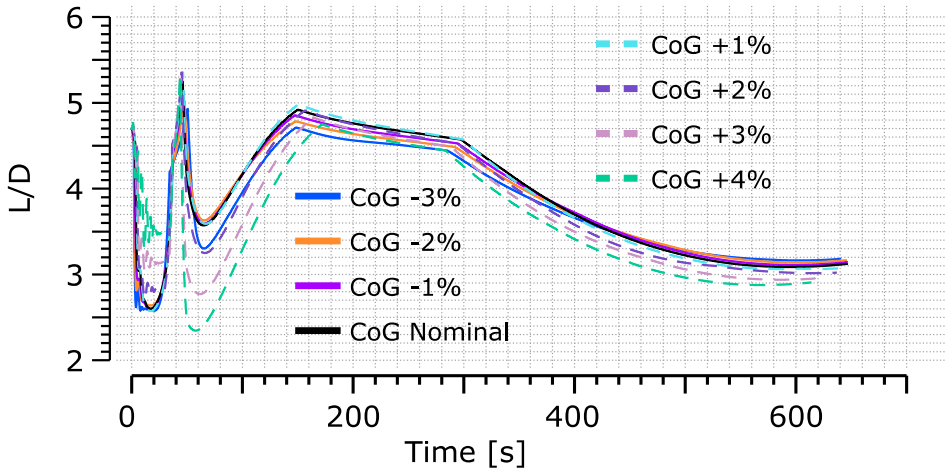

Fig 14. Aerodynamic efficiency of optimised trajectories for various CoG positions.

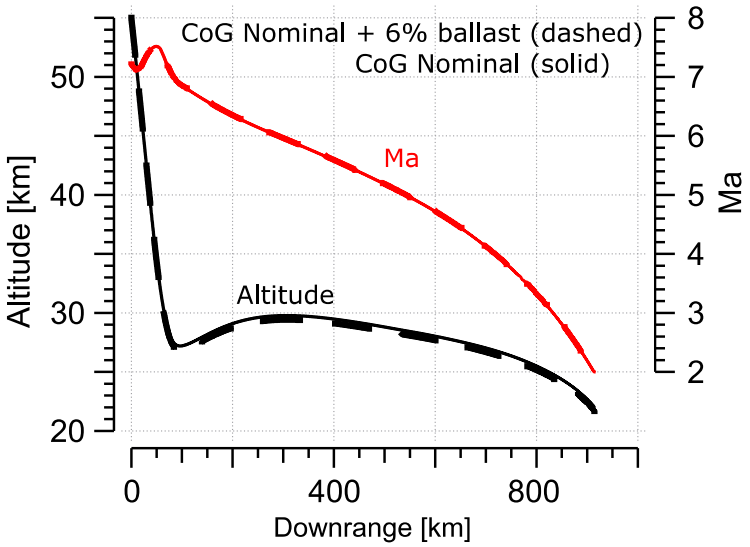

Fig 15. Altitude and Mach profiles of nominal and ballasted optimal trajectories.

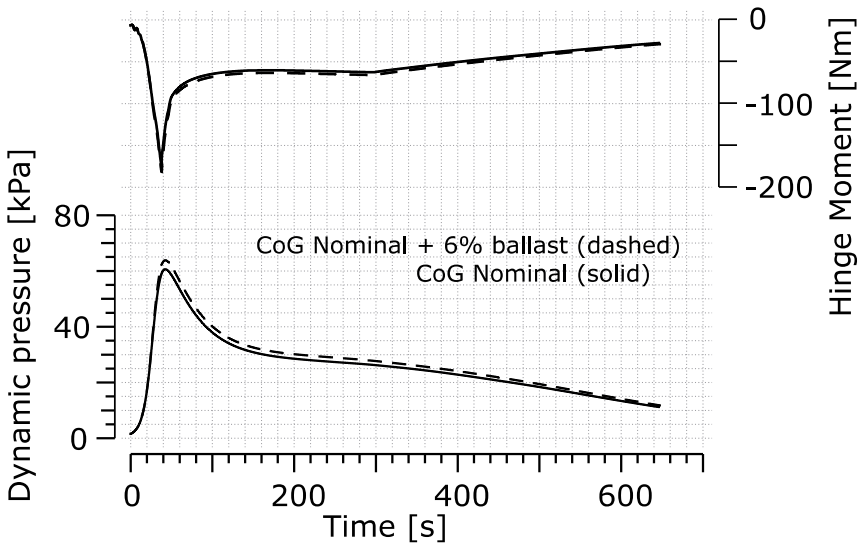

Fig 16. Dynamic pressure and elevator hinge moment profiles of nominal and ballasted optimal trajectories.

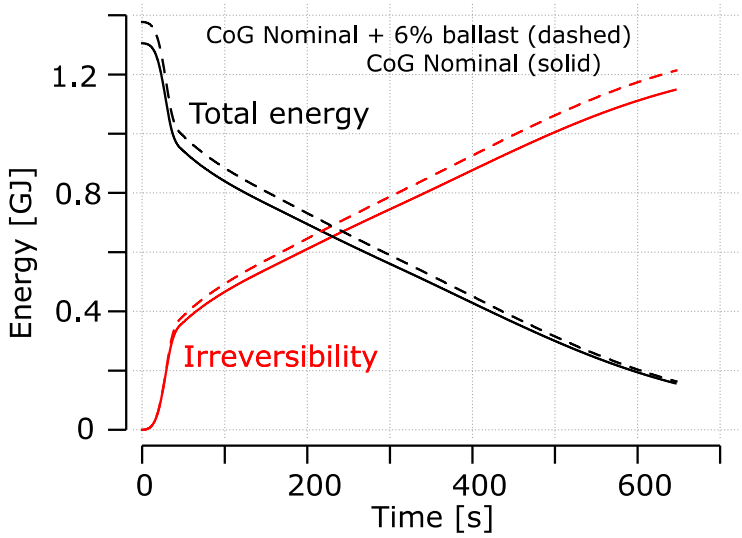

Fig 17. Vehicle total energy and cumulated irreversibility along nominal and ballasted optimal trajectories.

4. Conclusions

Drifts of +/-4% around the CoG show large penalties on the aerodynamic efficiency along the glider trajectory in the case of a constant pitch rate control. Whereas the forward displacement of CoG decreases the aerodynamic efficiency to about 2 and the flight time and downrange to respectively 30% and 25%, the impact of the backward drift is more benign for this particular initial conditions and flight control. The correction of each drift by a ballast mass increases 11% the vehicle mass and brings the trajectories back to the nominal one.

On the other hand, when the pitch command is optimised, a 4% CoG drift results in less than 5% downrange variation and a loss of less than 10% of aerodynamic efficiency during cruise and at the maximum efficiency peak: when the CoG drifts forward then the vehicle losses pull up command and plunges deeper into the denser atmosphere. On the other hand, the vehicle gains authority to fly at higher AoA when the CoG drifts backwards. A ballast of 6% corrects the CoG shift of 2%. The optimized trajectory for the ballasted vehicle is very close to the nominal, being the major difference a slight loss of altitude.

Acknowledgements

This work was performed within the 'High Speed Experimental Fly Vehicles - International' (HEXAFLYINT) project fostering International Cooperation on Civil High-Speed Air Transport Research. HEXAFLYINT, coordinated by ESA-ESTEC, is supported by the EU within the 7th Framework Program Theme 7 Transport, Contract no.: ACP3-GA-2014-620327. The project is also supported by the Ministry of Industry and Trade, Russian Federation. Further information on HEXAFLY-INT can be found on http://www.esa.int/techresources/hexafly_int.

References

1. J. Steelant et Al.: Flight Testing Designs in HEXAFLY-INT for High-Speed Transportation. In HiSST: International Conference on High-Speed Vehicle Science Technology, Moscow, 2018: 2018-3101064.
2. Takovitskii, S.A.: On the Role of a Balancing Load in the Problem of Aerodynamic Drag Minimization in the Supersonic Flight Regime. In Fluid Dynamics, 2014, Vol. 49, No. 2, pp. 238–248.
3. Schettino et Al.: Aerodynamic and Aerothermodynamic Database of the HEXAFLY-INT Hypersonic Glider. In HiSST: International Conference on High-Speed Vehicle Science Technology, Moscow, 2018.
4. Gutiérrez, B. G., Vara, R. P.: Building a flight mechanics library using EcosimPro. In 1st Meeting of EcosimPro Users, Madrid, 2001.